



Published in final edited form as:

Nature. 2015 May 21; 521(7552): 362–365. doi:10.1038/nature14442.

## Lipid nanoparticle siRNA treatment of Ebola virus Makona infected nonhuman primates

Emily P. Thi<sup>1,\*</sup>, Chad E. Mire<sup>2,3,\*</sup>, Amy C.H. Lee<sup>1</sup>, Joan B. Geisbert<sup>2,3</sup>, Joy Z. Zhou<sup>1</sup>, Krystle N. Agans<sup>2,3</sup>, Nicholas M. Snead<sup>1</sup>, Daniel J. Deer<sup>2,3</sup>, Trisha R. Barnard<sup>1</sup>, Karla A. Fenton<sup>2,3</sup>, Ian MacLachlan<sup>1</sup>, and Thomas W. Geisbert<sup>2,3,†</sup>

<sup>1</sup>Tekmira Pharmaceuticals, Burnaby, BC, Canada

<sup>2</sup>Galveston National Laboratory, University of Texas Medical Branch, Galveston, TX, USA

<sup>3</sup>Department of Microbiology and Immunology, University of Texas Medical Branch, Galveston, TX, USA

### Abstract

The current outbreak of Ebola virus (EBOV) in West Africa is unprecedented, causing more cases and fatalities than all previous outbreaks combined, and has yet to be controlled<sup>1</sup>. Several postexposure interventions have been employed under compassionate use to treat a number of patients repatriated to Europe and the United States<sup>2</sup>. However, the *in vivo* efficacy of these interventions against the new outbreak strain of EBOV is unknown. Here, we show that lipid nanoparticle (LNP)-encapsulated siRNAs rapidly adapted to target the Makona outbreak strain of EBOV are able to protect 100% of rhesus monkeys against lethal challenge when treatment was initiated at 3 days postexposure while animals were viremic and clinically ill. Although all infected animals showed evidence of advanced disease including abnormal hematology, blood chemistry, and coagulopathy, siRNA-treated animals had milder clinical features and fully recovered while the untreated control animals succumbed. These results represent the first successful demonstration of therapeutic anti-EBOV efficacy against the new outbreak strain in nonhuman primates (NHPs) and highlight the rapid development of LNP-delivered siRNA as a countermeasure against this highly lethal human disease.

---

Users may view, print, copy, and download text and data-mine the content in such documents, for the purposes of academic research, subject always to the full Conditions of use:[http://www.nature.com/authors/editorial\\_policies/license.html#terms](http://www.nature.com/authors/editorial_policies/license.html#terms)

<sup>†</sup>To whom correspondence should be addressed. [twgeisbe@utmb.edu](mailto:twgeisbe@utmb.edu).

\*These authors contributed equally to the manuscript.

**Author contributions:** E.T. and J.Z. designed the siRNA and did preparative work for DLR studies. E.T., N.S., J.Z. and A.L. designed the DLR studies. J.Z., T.B. and N.S. conducted the DLR studies and analyzed the data. E.T., C.E.M., A.L., I.M., and T.W.G. conceived and designed the NHP study. C.E.M., J.B.G., D.D., and T.W.G. performed the NHP challenge and treatment experiments and conducted clinical observations of the animals. J.B.G., K.N.A., and D.D. performed the clinical pathology assays. J.B.G. performed the EBOV Makona infectivity assays. C.E.M. and K.N.A. performed the PCR assays. E.T., C.E.M., J.B.G., K.N.A., D.D., K.A.F., A.L., I.M., and T.W.G. analyzed the data. K.A.F. performed histologic and immunohistochemical analysis of the data. E.T., C.M., A.L. and T.W.G. wrote the paper. All authors had access to all of the data and approved the final version of the manuscript.

**Competing interests:** A.L., I.M., and T.W.G. claim intellectual property regarding RNA interference for the treatment of filovirus infections. I.M. and T.W.G. are co-inventors on US Patent 7,838,658 “siRNA silencing of filovirus gene expression” and A.L., I.M., and T.W.G. are co-inventors on US Patent 8,716,464 “Compositions and methods for silencing Ebola virus gene expression”. The other authors declare no competing interests. Opinions, interpretations, conclusions, and recommendations are those of the authors and are not necessarily endorsed by the University of Texas Medical Branch.

Historical EBOV outbreaks have previously ranged in size from a few to over 400 cases and were relatively well controlled by contact tracing and quarantine methods. In late 2013, an unprecedented outbreak caused by the Zaire species of EBOV began. This outbreak focused around the West African countries of Guinea, Liberia, and Sierra Leone and has continued unabated for over a year to date with 24,957 cases and 10,350 deaths<sup>1</sup>. Despite intensive containment efforts, the outbreak is still not under control and the need for medical countermeasures to both prevent and treat infections has never been greater.

While there are no approved vaccine or therapeutic treatment modalities available for preventing or managing EBOV infections, a few postexposure approaches have demonstrated convincing efficacy against EBOV in a NHP model which closely reproduces human infection. These include anti-EBOV monoclonal antibody administration alone (such as ZMapp) or with adenovirus-vectored interferon- $\alpha$ , and EBOV-targeting siRNAs encapsulated in LNPs (TKM-Ebola) to potentiate cellular delivery<sup>3-5</sup>. A number of experimental treatments including ZMapp and TKM-Ebola have been employed under compassionate use protocols to treat small numbers of repatriated EBOV-infected medical staff in Europe and the United States<sup>2</sup>. However, the contribution of these experimental treatments towards patient survival cannot be established, as multiple experimental treatments were applied in parallel alongside aggressive supportive care. Clinical trials have been initiated in West Africa to evaluate the efficacy of a number of experimental treatments including convalescent serum, vaccines, small molecules (brincidovir now halted) and recently ZMapp although these investigations may become hampered by the dwindling number of new cases of infection. Further, up to now no treatments have been tested against the current outbreak strain of EBOV under experimentally well-controlled conditions. As much of the prior vaccine and antiviral development has been conducted in NHPs using the historical EBOV 1995 Kikwit strain from Central Africa, there is a possibility that sequence changes documented in the West African strain<sup>6-8</sup> may interfere with medical countermeasure efficacy, highlighting the need for treatments that can be rapidly adapted to mutated etiological agents. While siRNA recognition is sequence dependent, adjustments for small viral nucleotide changes can be made rapidly. Monoclonal antibodies rely on cross-reactivity to conserved epitopes; if these are significantly changed, suitable antibodies must be identified *de novo*.

Sequence alignments of the nucleotide target sites of the TKM-Ebola siRNA cocktail, siEbola-2, with available sequences from the West African outbreak<sup>6-8</sup> revealed conserved mismatches at antisense position 6 for siLpol-2 and at positions 3 and 15 for siVP35-2 that are not present in virus sequences endemic to Central Africa (Fig. 1a). While certain positions within the prototypical siRNA structure are considered more critical for function, and others better able to tolerate mismatches without erosion of activity, such effects are sequence-dependent and difficult to predict<sup>9-12</sup>. Given this uncertainty, we took advantage of the rapid adjustment capability of the siRNA-LNP platform and designed a new siRNA cocktail, siEbola-3, in which these mismatches were corrected to enable full complementarity to West African outbreak EBOV sequences. We utilized a virus-free dual luciferase reporter (DLR) assay to model the gene silencing ability of the adjusted siRNA components against a representative Central African strain versus the West African strain. Results demonstrated that the new siEbola-3 cocktail is fully active against the West African

EBOV sequence, and retains activity against the Central African sequence despite an impairment of the siVP35-3 siRNA component (Fig. 1b, see also Methods).

In order to assess medical countermeasure antiviral efficacy against the West African EBOV strain, we employed *in vitro* and rhesus macaque models using a virus isolate from a lethal case in Guinea<sup>6</sup>. Deep sequencing of the challenge stock confirmed viral identity with 100% of the sequences containing the wild type phenotype of 7 consecutive template uridines (7U) at the glycoprotein editing site confirming that viral virulence was not compromised during preparation of the challenge stock<sup>13,14</sup>. It has been shown that macaques infected with 7U EBOV Kikwit succumb to infection earlier than those infected with 8U virus, and the protection afforded by some vaccine candidates decreases with EBOV 7U infection<sup>15,16</sup>. Consistent with DLR predictions, both siEbola-2 and siEbola-3 LNPs were able to inhibit viral RNA levels in cultured cells infected with either EBOV Makona or EBOV Kikwit although the siRNAs with full complementarity resulted in more activity (Ext. Data Fig. 1).

siEbola-3 LNP treatment was able to protect NHPs against lethal challenge. NHPs were infected with the West African EBOV isolate and either left as untreated controls or administered siEbola-3 LNP beginning at 72 h after infection when animals were viremic and clinically ill. All treated animals survived to study endpoint while untreated control animals succumbed on days 8 and 9 (Fig. 2a). The time-to-death observed in untreated animals was similar to that reported upon symptom onset in patients ( $9.8 \pm 0.7$  days<sup>17</sup>), suggesting that EBOV infection in NHPs closely reproduces this aspect of human infection. Untreated control animals displayed mild clinical signs up until the day of euthanasia, upon which a rapid deterioration of condition necessitated euthanasia (Fig. 2b). This is somewhat different from the disease course observed in NHPs infected with the EBOV Kikwit strain, where animals tend to show a more gradual decline over the course of 1–3 days (Ext. Data Table 1)<sup>3,18,19</sup>. In contrast to control animals, all siEbola-3 LNP-treated animals developed only transient mild clinical symptoms (Fig. 2b). Fever was observed in all infected animals with the exception of one treated animal, beginning at day 5 or 6 and continuing for 2–3 days until temperature returned to baseline (treated animals) or animals became hypothermic (Table 1). Petechial rashes were observed in all untreated and two treated animals, and these were milder than that seen previously in animals infected with EBOV Kikwit<sup>3,16,17</sup>. Severe diarrhea was also observed in two untreated animals infected with EBOV Makona, a clinical symptom associated with a fatal outcome in patients from this outbreak<sup>15</sup>. Diarrhea is not as commonly observed in NHPs infected with EBOV Kikwit (T.W. Geisbert, unpublished observations). Taken together, these observations suggest that siEbola-3 LNP treatment protects against lethal EBOV Makona infection in a NHP model that recapitulates aspects of the disease observed in patients in the current West African outbreak, and that the disease manifestation in NHPs infected with EBOV Makona may differ from EBOV Kikwit infection.

siEbola-3 LNP treatment was also able to reduce viral load in infected animals (1–4 log unit reductions in plasma viremia when compared to control animals, Fig. 2c), which correlated with 7.6- to 114-fold decreases in circulating viral genome detection (Fig. 2d, day 6). Peak viral RNA levels in untreated control animals were 8 and 9 log copies/mL, respectively, well over the 10 million EBOV copies/mL threshold associated with a higher fatality rate in

patients<sup>17</sup>. At euthanasia, viral RNA was also widespread in tissues of untreated control animals whereas it was only detected in lymph nodes and spleen of treated animals at levels that were several magnitudes lower (Fig. 2e). These tissues were negative for infectious virus by plaque assay (data not shown), suggesting that the presence of viral RNA was not due to incomplete viral clearance. However, viral RNA detection at study endpoint in these sites of antigen presentation may reflect enforced viral replication in antigen presenting cells, which allows for adequate amounts of antigen to be presented to promote the adaptive immunity critical for survival after infection with a cytopathic virus<sup>20</sup>. In accordance with this, immunohistochemical tissue evaluation showed positive EBOV antigen staining for the untreated control animals consistent with historical EBOV Kikwit-infected macaques<sup>3,18,19</sup> whereas detection of EBOV antigen in tissues of the fully recovered siEbola-3 LNP-treated animals was rare and limited to cells associated with antigen presentation (Figure 3). No difference in viremia levels was observed between EBOV Makona and historical Kikwit infected animals based on limited available data (Ext. Fig. 2a).

In conjunction with reductions in viral load, animals treated with siEbola-3 LNP displayed moderate protection against liver dysregulation seen in untreated control animals infected with EBOV Makona, although the level of disturbance observed in infected animals was not as dramatic as those seen historically in rhesus macaques infected with EBOV Kikwit (Ext. Fig. 2b–e). Treated animals also displayed protection against EBOV-induced renal dysfunction as assessed by creatinine and BUN levels (Ext. Fig. 2f, g). Smaller differences in coagulopathy, lymphopenia, and thrombocytopenia were observed between treated and untreated animals (Table 1, Ext. Fig. 3). No differences in these parameters were apparent in untreated animals after infection with either EBOV Makona or EBOV Kikwit. Overall, these results suggest that siEbola-3 LNP treatment may confer additional protective benefits against clinical symptoms of EBOV-induced disease in addition to its survival advantage and effective control of viral load. Some clinical pathology characteristics such as liver dysfunction were found to be not as profound in EBOV Makona-infected NHPs when compared to that observed previously for EBOV Kikwit infection.

The current EBOV outbreak in West Africa highlights the need for antiviral therapeutics and prophylactics that can be readily and rapidly adapted to address the changing viral strain landscape. The use of a cocktail format (as opposed to a single siRNA) increases the likelihood of activity retention against newly emergent viral strains, as evidenced by the activity of siEbola-2 against EBOV Makona despite the presence of several nucleotide mismatches (Fig 1b, Ext. Data Fig. 1). Further, the bipartite structure of TKM-Ebola, comprising both siRNA and LNP, allows for adjustments to the siRNA component in order to capitalize on emerging strain sequence data while maintaining the delivery functionality of the LNP component. Once viral sequence data is available, clinical grade drug product can be produced in as little as 8 weeks. Although TKM-Ebola specific for Central African EBOV is currently under a US FDA partial clinical hold regarding the treatment of healthy uninfected subjects, this therapeutic candidate has been cleared by the FDA for use in EBOV-infected patients, with the acknowledgment that the risk:benefit profile is quite different for EBOV-infected individuals facing a high mortality rate compared to healthy uninfected volunteers. The new siEbola-3 siRNA cocktail, shown here to possess robust

activity against the latest EBOV Makona outbreak strain, is now being evaluated for efficacy in EBOV-infected patients in Sierra Leone, West Africa.

## Methods

### Dual luciferase reporter assay

The psiCHECK2 (Promega) vector was used to construct the EBOV Makona and EBOV Kikwit strain reporter plasmids used in this study (Genscript). Briefly, to construct the EBOV Makona or EBOV Kikwit reporter plasmids, two 201 bp regions of either the EBOV Makona strain or EBOV Kikwit strain genomes containing the VP35 and Lpol target sites (nucleotide positions 17287 to 17488, and 3817 to 4018 of Genbank accession no. KJ660347.2 or AY354458) were fused together and cloned into the 3' UTR of the Rluc gene between the XhoI and NotI restriction sites to allow for the detection of siRNA activity as represented by decreased Rluc activity. siLpol-3 and siVP35-3 were synthesized at ST Pharm Co. and siLpol-2 and siVP35-2 were synthesized at Integrated DNA Technologies. Individual duplexes and the siEbola-3 or siEbola-2 cocktail (1:1 molar mixture of siLpol-3 and siVP35-3 or siLpol-2 and siVP35-2, respectively) were encapsulated in LNP by the process of spontaneous vesicle formation as previously reported<sup>21</sup>. The resulting LNPs were dialyzed against PBS and sterilized through a 0.2 µm filter before use. siRNAs targeting Renilla luciferase and MARV NP (synthesized by Integrated DNA Technologies) were also encapsulated in LNP and were included as positive and negative controls, respectively.

Authenticated HepG2 cells were obtained from ATCC (ATCC HB-8065). The cells were not tested for mycoplasma. HepG2 cells were transfected with the EBOV Makona or EBOV Kikwit psiCHECK2 plasmid construct using Lipofectamine 2000 (Life Technologies) and treated with siRNA-LNP at 5, 50, 125, 250, 500 and 750 ng/mL. Transfected cells were incubated for 24 hours, followed by measurement of Renilla and firefly luciferase activities using a luminometer. Results were expressed as a percentage of the Renilla:firefly luciferase activity in cells transfected with the reporter plasmid only (no siRNA treatment).

### EBOV Makona virus and sequence analysis

The EBOV Makona strain seed stock originated from serum from a fatal case during the 2014 outbreak in Guékédou, Guinea (*Zaire ebolavirus* isolate H.sapiens-wt/GIN/2014/Makona-Gueckedou-C07, accession number KJ660347.2)<sup>6</sup> and was passaged twice in authenticated Vero E6 cells obtained from ATCC (ATCC, CRL-1586). The cells were not tested for mycoplasma. The EBOV Makona strain passage 2 seed stock was extracted in Trizol LS (Invitrogen) then purified using Zymo Research Direct-zol RNA mini-prep (Zymo Research) per manufacturer's instructions. cDNA was generated from purified RNA using the Ovation RNA-seq 2 kit which was subsequently used for the preparation of the double stranded DNA library using the Encore Ion Torrent library prep kit (NuGen). Sequencing was performed by the UTMB Molecular Core on the Ion Torrent using 318-v2 deep sequencing chips. Sequence analysis was performed using Seqman NGen software (DNA Star) based on paired-end analysis of 100 base pair overlaps.

### In vitro infections

HepG2 cells (ATCC HB-8065) were seeded at  $1 \times 10^5$  cells/well in 24-well culture plates and incubated at  $37^\circ\text{C}/5\% \text{CO}_2$  overnight prior to infection with 0.1 MOI of either EBOV Makona or Kikwit. Cells were incubated with virus for 1 h, then washed four times with PBS and treated with siRNA-LNP at 51.2, 6.4 and 0.8 ng/mL. Cells were incubated for 48 h post-treatment prior to harvesting of cell supernatants for RNA extraction by Trizol and qRT-PCR assessment.

### Animal challenge

Six healthy adult rhesus macaques (*Macaca mulatta*) of Chinese origin (4–8 kg, three males and three females, 4–8 years old) were inoculated intramuscularly (i.m.) with 1,000 pfu of EBOV Makona strain. The historical EBOV Kikwit data was obtained from six healthy rhesus macaques (six females, 4–8 years old) inoculated i.m. with 1,000 pfu of EBOV Kikwit strain. Sample sizes were based on the availability of rhesus macaques. Animals were randomized with Microsoft Excel into treatment or control groups. siEbola-3 LNP (0.5 mg/kg) was administered to three of the EBOV Makona-infected macaques by bolus i.v. infusion 72 hours after EBOV challenge while the control animals were not treated. The three treated animals received additional treatments of siEbola-3 LNP on days 4, 5, 6, 7, 8, and 9 after EBOV challenge. All animals (six infected with EBOV Makona and six infected with EBOV Kikwit) were given physical exams and blood was collected at the time of challenge and on days 3, 6, 10, 14, 22, and 28 after EBOV challenge or at time of euthanasia. In addition, all animals were monitored daily and scored for disease progression with an internal filovirus scoring protocol approved by the UTMB Institutional Animal Care and Use Committee. The scoring changes measured from baseline included posture/activity level, attitude/behavior, food and water intake, weight, respiration, and disease manifestations such as visible rash, hemorrhage, ecchymosis, or flushed skin. A score of 9 indicated that an animal met criteria for euthanasia. This study was not blinded.

### Detection of viremia and viral RNA

RNA was isolated from whole blood or tissues utilizing the Viral RNA Mini Kit or RNeasy Kit (Qiagen) using 100  $\mu\text{L}$  of blood into 600  $\mu\text{L}$  of buffer AVL, or 100 mg of tissue per manufacturer's instructions, respectively. Primers/probe targeting the VP30 gene of EBOV were used for quantitative real-time PCR (qRT-PCR) with the probe used here being 6-carboxyfluorescein (6FAM)- 5'- CCG TCA ATC AAG GAG CGC CTC 3' - 6-carboxytetramethylrhodamine (TAMRA) for the EBOV Makona NHP and EBOV Makona and Kikwit in vitro studies (Life Technologies). EBOV RNA was detected using the CFX96 detection system (BioRad Laboratories) in One-step probe qRT-PCR kits (Qiagen) with the following cycle conditions:  $50^\circ\text{C}$  for 10 minutes,  $95^\circ\text{C}$  for 10 seconds, and 40 cycles of  $95^\circ\text{C}$  for 10 seconds and  $59^\circ\text{C}$  for 30 seconds. Threshold cycle (CT) values representing EBOV genomes were analyzed with CFX Manager Software, and data are shown as means  $\pm$  SD of technical replicates. To create the GEq standard, RNA from EBOV stocks was extracted and the number of EBOV genomes calculated using Avogadro's number and the molecular weight of the EBOV genome.

Virus titration was performed by plaque assay with Vero E6 cells from all serum samples as previously described<sup>3,16,17</sup>. Briefly, increasing 10-fold dilutions of the samples were adsorbed to Vero E6 monolayers in duplicate wells (200  $\mu$ L); the limit of detection was 5 pfu/mL.

### **Hematology, serum biochemistry, and blood coagulation**

Total white blood cell counts, white blood cell differentials, red blood cell counts, platelet counts, hematocrit values, total hemoglobin concentrations, mean cell volumes, mean corpuscular volumes, and mean corpuscular hemoglobin concentrations were analyzed from blood collected in tubes containing EDTA using a laser based hematologic analyzer (Beckman Coulter). Serum samples were tested for concentrations of albumin, amylase, alanine aminotransferase (ALT), aspartate aminotransferase (AST), alkaline phosphatase (ALP), gamma-glutamyltransferase (GGT), glucose, cholesterol, total protein, total bilirubin (TBIL), blood urea nitrogen (BUN), creatinine (CRE), and C-reactive protein (CRP) by using a Piccolo point-of-care analyzer and Biochemistry Panel Plus analyzer discs (Abaxis). Citrated plasma samples were analyzed for coagulation parameters prothrombin time (PT), activated partial thromboplastin time (APTT), and fibrinogen on the STart4 instrument using the PTT Automate, STA Neoplastine CI plus, and Fibri-Prest Automate, kits, respectively (Diagnostica Stago).

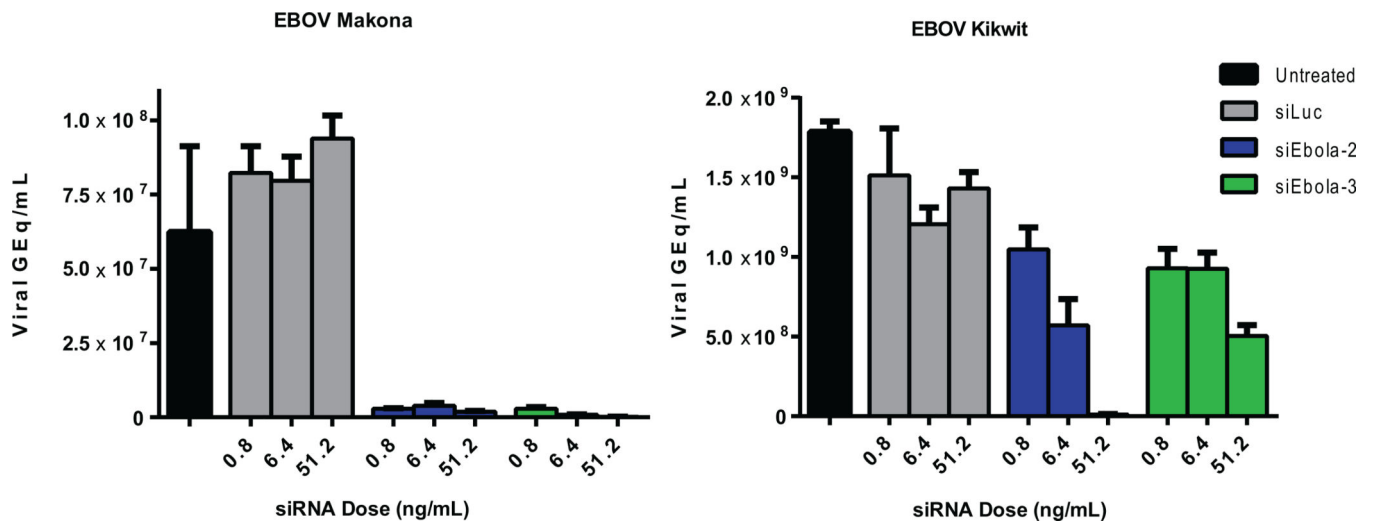
### **Histopathology and immunohistochemistry**

Necropsy was performed on all subjects. Tissue samples of all major organs were collected for histopathologic and immunohistochemical examination, immersion-fixed in 10% neutral buffered formalin, and processed for histopathology as previously described<sup>16,17</sup>. For immunohistochemistry, specific anti-EBOV immunoreactivity was detected using an anti-EBOV VP40 protein rabbit primary antibody (Integrated BioTherapeutics) at a 1:4000 dilution. In brief, tissue sections were processed for immunohistochemistry using the Dako Autostainer (Dako). Secondary antibody used was biotinylated goat anti-rabbit IgG (Vector Laboratories) at 1:200 followed by Dako LSAB2 streptavidin-HRP (Dako). Slides were developed with Dako DAB chromagen (Dako) and counterstained with hematoxylin. Non-immune rabbit IgG was used as a negative control. Liver, adrenal gland, and inguinal lymph nodes representative images were taken at 40 $\times$ , and spleen taken at 20 $\times$  from control animal 0805068 (**A, E, H, and M**) or treated animals 0902056 (**B, F, J, and N**), 1005445 (**C, G, K, and O**), and 1006421 (**D, H, L, and P**).

### **Statistical Analyses**

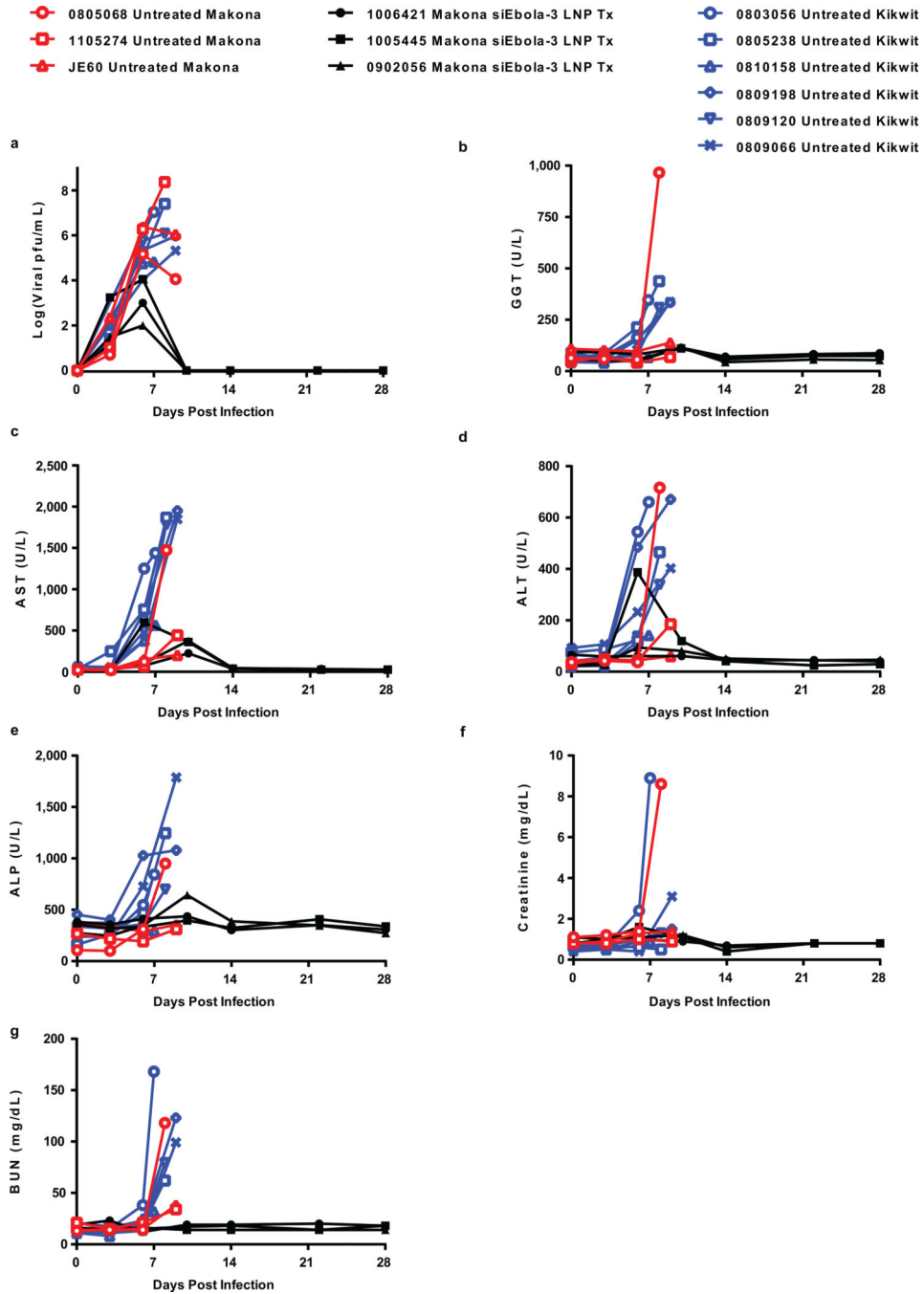
Analysis was conducted with Graphpad Prism software (version 6.04). A paired t-test (one-sided) was used to compare untreated and treated group means on day 6 for qRT-PCR (untreated group mean  $\pm$  SD was 8.51 log GEq/mL  $\pm$  0.74; siEbola-3 LNP treated group was 6.36 log GEq/mL  $\pm$  0.62) and viremia (untreated group mean  $\pm$  SD was 5.94 log (pfu/mL)  $\pm$  0.67; siEbola-3 LNP treated group was 3.02 log (pfu/mL)  $\pm$  1.03).

## Extended Data



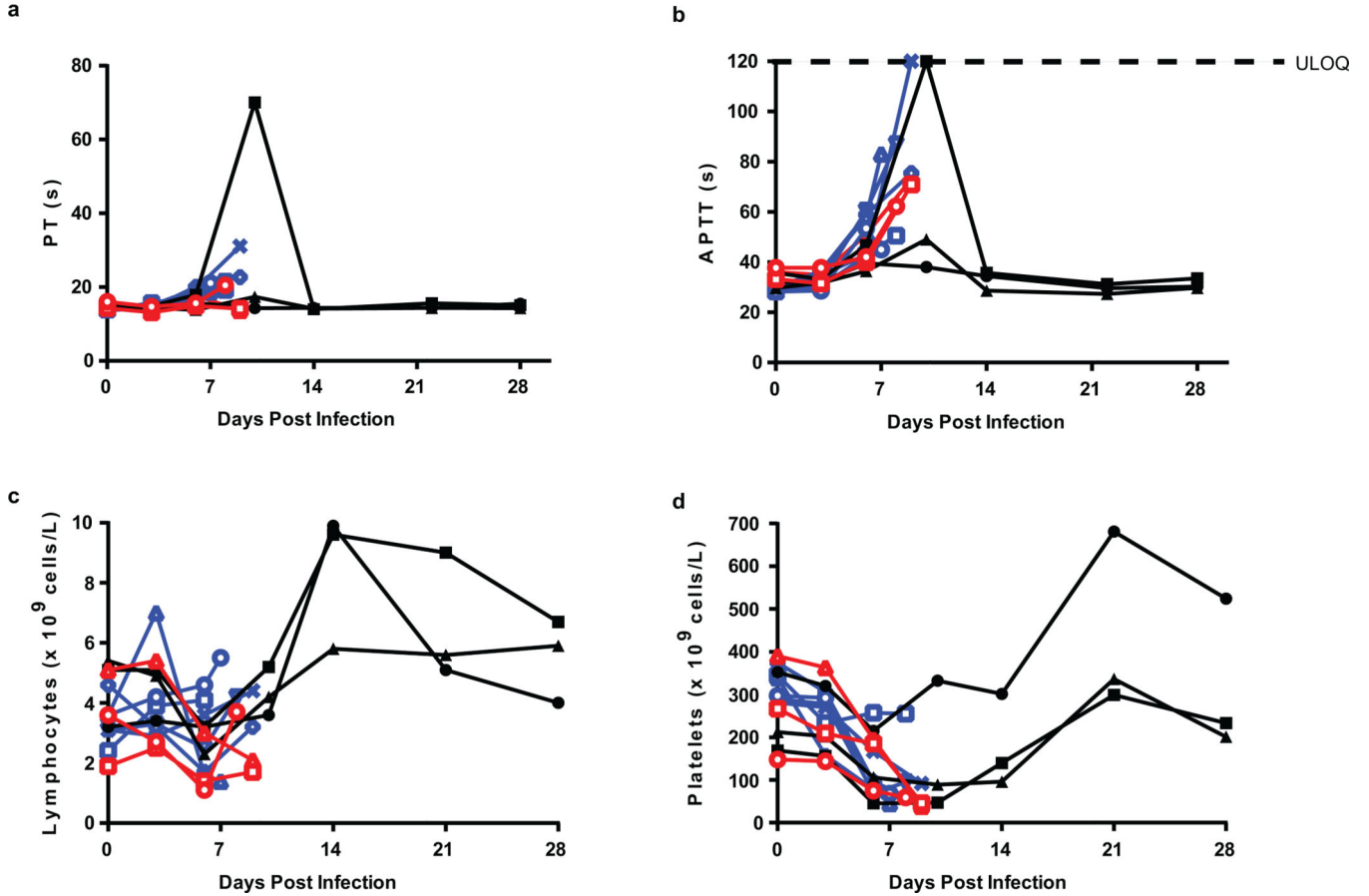
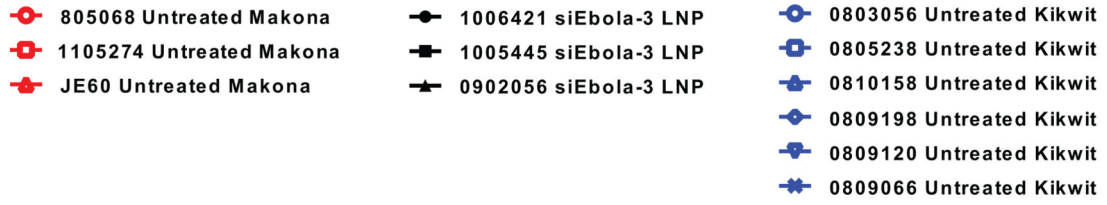
**Extended Data Figure 1. Antiviral activity of siEbola-3 in cells infected with EBOV Makona**  
 For comparison, siEbola-3 activity was also assessed against the Central African EBOV Kikwit strain and siEbola-2 activity was evaluated against both EBOV strains. Data is viral RNA copies/mL of each sample normalized to untreated infected cells. Results are mean  $\pm$  SD from one biological replicate, conducted in technical triplicate.





**Extended Data Figure 2. siEbola-3 LNP treatment provides partial protection against EBOV Makona clinical pathologies, and infection with EBOV Makona infection induces a lesser degree of liver dysfunction compared to EBOV Kikwit infection**

**a.** No differences in viremia levels were observed in untreated animals infected with EBOV Makona or Kikwit. **b–e.** Liver dysfunction markers. Normal values for uninfected NHPs ranges are GGT (40–115 U/L), AST (20–45 U/L), ALT (20–165 U/L), ALP (130–500 U/L). **f, g.** Protection against EBOV Makona-induced CRE and BUN elevation was observed. Normal values for uninfected NHPs range from BUN (10–25 mg/dL) and CRE (0.8–1.2 mg/dL).



**Extended Data Figure 3. Comparison of coagulation and hematology characteristics between untreated control animals infected with EBOV Makona or Kikwit**

**a, b.** Coagulopathies are not as marked in EBOV Makona infection when compared to historical EBOV Kikwit data. **c.** Lymphopenia is observed in all infected animals. **d.** Thrombocytopenia levels are similar between EBOV Makona and EBOV Kikwit infected control animals.

**Extended Data Table 1**

Comparison of clinical signs progression between untreated rhesus macaques infected with EBOV Makona or EBOV Kikwit.

Infection	Animal ID	Day 1	Day 2	Day 3	Day 4	Day 5	Day 6	Day 7	Day 8	Day 9
EBOV Makona	1105274	0	0	0	0	0	0	0	1	16
	0805068	0	0	0	0	0	1	1	15	

Infection	Animal ID	Day 1	Day 2	Day 3	Day 4	Day 5	Day 6	Day 7	Day 8	Day 9
	JE60	0	0	0	0	0	1	3	3	14
	809066	0	0	0	0	0	0	0	0	11
	809120	0	0	0	0	0	1	2	17	
EBOV Kikwit	809198	0	0	0	1	1	1	1	3	11
	810158	0	0	0	0	1	1	10		
	805238	0	0	0	0	1	1	14		
	803056	0	0	0	0	0	1	1	10	

## Acknowledgments

We thank Dr. Viktoria Borisevich for assistance with clinical pathology assays performed in the GNL BSL-4 laboratory. We also thank Shaun Klassen for his assistance with siRNA-LNP preparation.

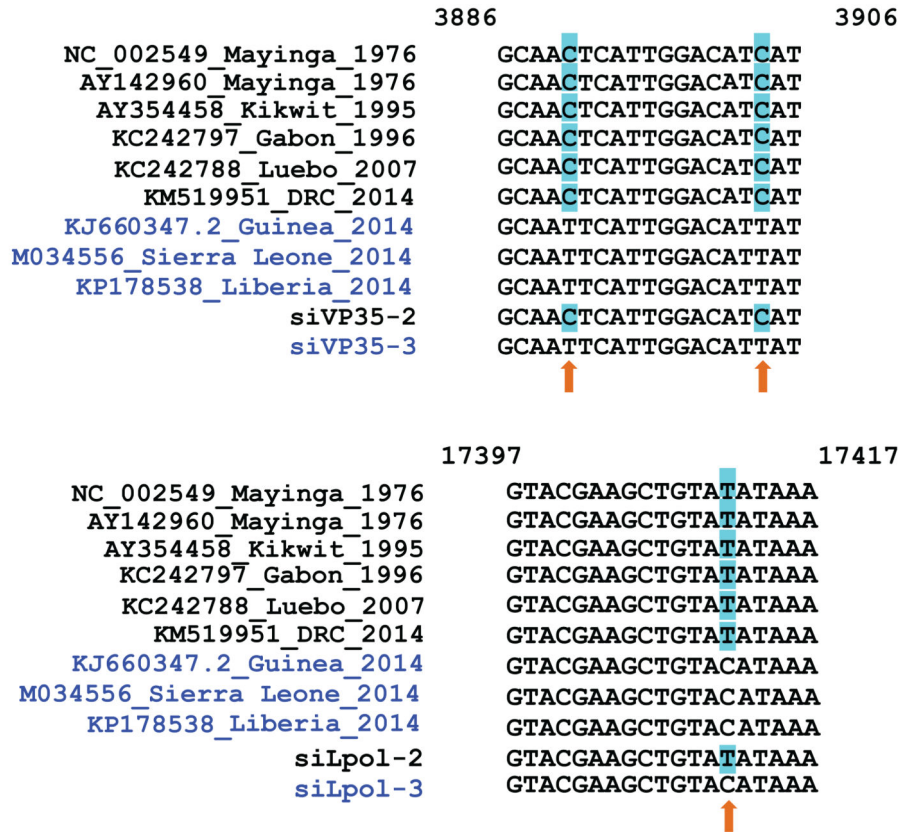
**Funding:** This study was supported by the Department of Health and Human Services, National Institutes of Health grant U19AI109711 to T.W.G. and I.M.

## References

1. World Health Organization. Ebola Data and Statistics. 2015. <<http://apps.who.int/gho/data/view ebola-sitrep ebola-summary-20150122?lang=en>>
2. Bishop BM. Potential and emerging treatment options for Ebola virus disease. *Ann Pharmacother*. 2015; 49:196–206. [PubMed: 25414384]
3. Geisbert TW, et al. Postexposure protection of non-human primates against a lethal Ebola virus challenge with RNA interference: a proof-of-concept study. *Lancet*. 2010; 375:1896–1905. [PubMed: 20511019]
4. Qiu X, et al. Reversion of advanced Ebola virus disease in nonhuman primates with ZMapp. *Nature*. 2014; 514:47–53. [PubMed: 25171469]
5. Qiu X, et al. mAbs and Ad-vectored IFN-alpha therapy rescue Ebola-infected nonhuman primates when administered after the detection of viremia and symptoms. *Sci Transl Med*. 2013; 5:207ra143.
6. Baize S, et al. Emergence of Zaire Ebola virus disease in Guinea. *N Engl J Med*. 2014; 371:1418–1425. [PubMed: 24738640]
7. Gire SK, et al. Genomic surveillance elucidates Ebola virus origin and transmission during the 2014 outbreak. *Science*. 2014; 345:1369–1372. [PubMed: 25214632]
8. Kugelman JR, et al. Evaluation of the potential impact of ebola virus genomic drift on the efficacy of sequence-based candidate therapeutics. *mBio*. 2015; 6
9. Du Q, Thonberg H, Wang J, Wahlestedt C, Liang Z. A systematic analysis of the silencing effects of an active siRNA at all single-nucleotide mismatched target sites. *Nucleic Acids Res*. 2005; 33:1671–1677. [PubMed: 15781493]
10. Schwarz DS, et al. Designing siRNA that distinguish between genes that differ by a single nucleotide. *PLoS genetics*. 2006; 2:e140. [PubMed: 16965178]
11. Huang H, et al. Profiling of mismatch discrimination in RNAi enabled rational design of allele-specific siRNAs. *Nucleic Acids Res*. 2009; 37:7560–7569. [PubMed: 19815667]
12. Dallas A, et al. Inhibition of hepatitis C virus in chimeric mice by short synthetic hairpin RNAs: sequence analysis of surviving virus shows added selective pressure of combination therapy. *J Virol*. 2014; 88:4647–4656. [PubMed: 24478422]
13. Volchkova VA, Dolnik O, Martinez MJ, Reynard O, Volchkov VE. Genomic RNA editing and its impact on Ebola virus adaptation during serial passages in cell culture and infection of guinea pigs. *J Infect Dis*. 2011; 204(Suppl 3):S941–S946. [PubMed: 21987773]

14. Kugelman JR, et al. Ebola virus genome plasticity as a marker of its passaging history: a comparison of in vitro passaging to non-human primate infection. *PLoS One*. 2012; 7:e50316. [PubMed: 23209706]
15. Trefry C, et al. *In vivo* Pathological Consequences of Ebola Virus Genome Plasticity: Is a 7U Virus More Lethal? American Society for Microbiology Biodefense and Emerging Diseases Research Meeting. Presentation. 2015; 164(A)
16. Hirschberg R, et al. Challenges, Progress, and Opportunities: Proceedings of the Filovirus Medical Countermeasures Workshop. *Viruses*. 2014; 6:2673–2697. [PubMed: 25010768]
17. Schieffelin JS, et al. Clinical illness and outcomes in patients with Ebola in Sierra Leone. *N Engl J Med*. 2014; 371:2092–2100. [PubMed: 25353969]
18. Geisbert TW, et al. Treatment of Ebola virus infection with a recombinant inhibitor of factor VIIa/tissue factor: a study in rhesus monkeys. *Lancet*. 2003; 362:1953–1958. [PubMed: 14683653]
19. Hensley LE, et al. Recombinant human activated protein C for the postexposure treatment of Ebola hemorrhagic fever. *J Infect Dis*. 2007; 196(Suppl 2):S390–S399. [PubMed: 17940975]
20. Honke N, et al. Enforced viral replication activates adaptive immunity and is essential for the control of a cytopathic virus. *Nat Immunol*. 2012; 13:51–57. [PubMed: 22101728]
21. Ma H, et al. Formulated Minimal-Length Synthetic Small Hairpin RNAs Are Potent Inhibitors of Hepatitis C Virus in Mice With Humanized Livers. *Gastroenterology*. 2014; 146:63–66. e65. [PubMed: 24076507]

**a**



**b**

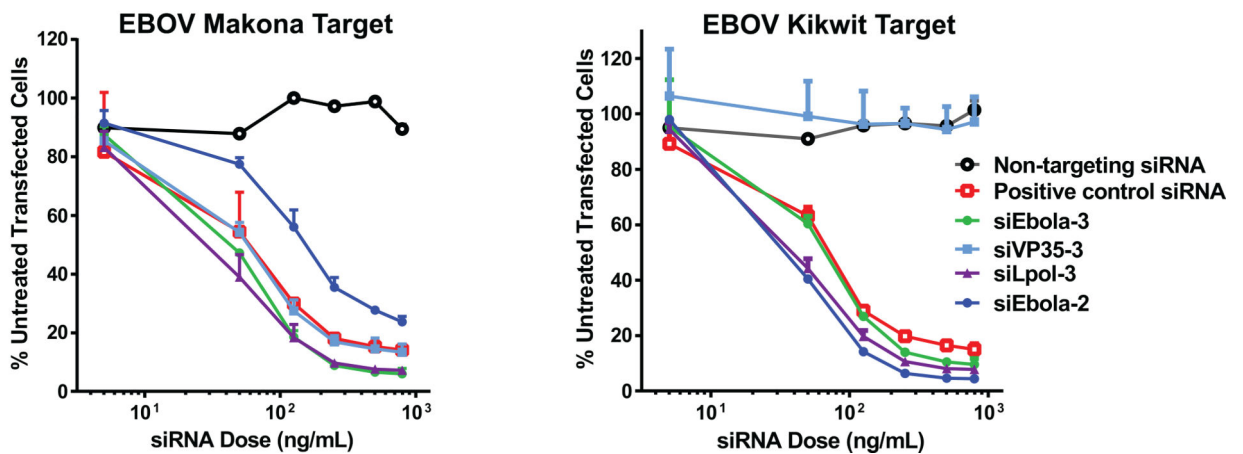


**Figure 1. siEbola-3 is active against EBOV Makona target sequences**

**a.** The TKM-Ebola siRNA cocktail of siVP35-2 and siLpol-2 targets gene regions in Central African EBOV sequences but West African outbreak sequences contain mutations at these locations. siEbola-3 has these target site mismatches corrected. **b.** siEbola-3 and its individual components, siVP35-3 and siLpol-3, are active against EBOV Makona sequences. Activity was assessed by dual luciferase reporter assay (see Methods). Shown is RLuc/FLuc of each sample normalized to untreated cells. Results are mean ± SEM from one (negative control) or two biological replicates (other data), conducted in technical triplicate.

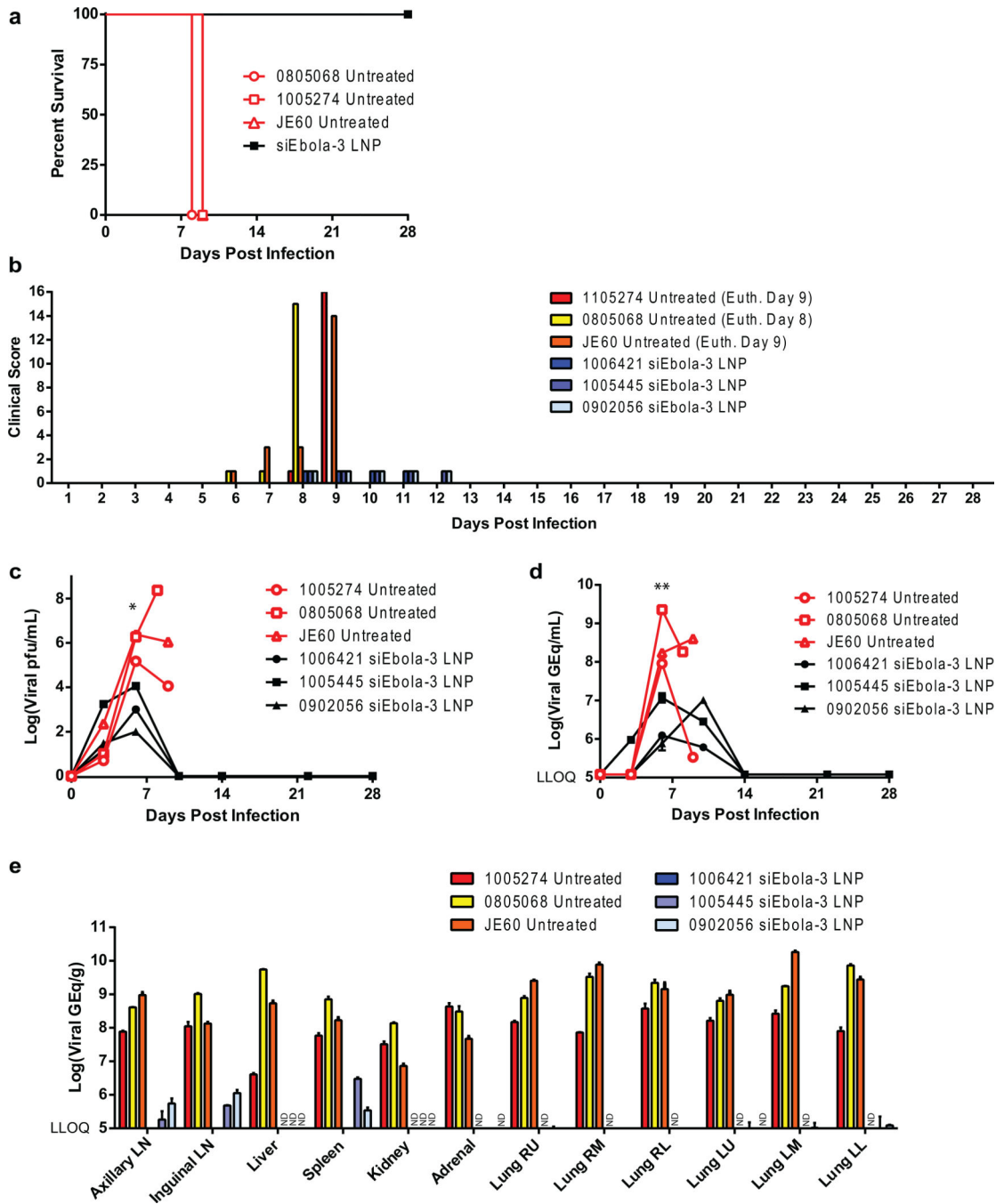


**Figure 2. siEbola-3 LNP treatment confers survival and reduces viral load**  
**a.** NHPs lethally challenged with EBOV Makona survive when treated with siEbola-3 LNP starting 72 h post-infection. **b.** Clinical signs were improved in treated animals. Treatment reduces **c.** infectious virus load (\* $p=0.0450$ , one-sided t-test, day 6) and **d.** viral RNA in blood (\*\* $p=0.0023$ , one-sided t-test, day 6); **e.** tissues. Lower limit of detection is 5 pfu/mL. **d., e.** qRT-PCR data shown are means  $\pm$  SD of two technical replicates. ND = Not detected. LLOQ = Lower limit of quantitation, 4.8 log<sub>10</sub> copies/g or 5.1 log<sub>10</sub> copies/mL. N = 3/group.

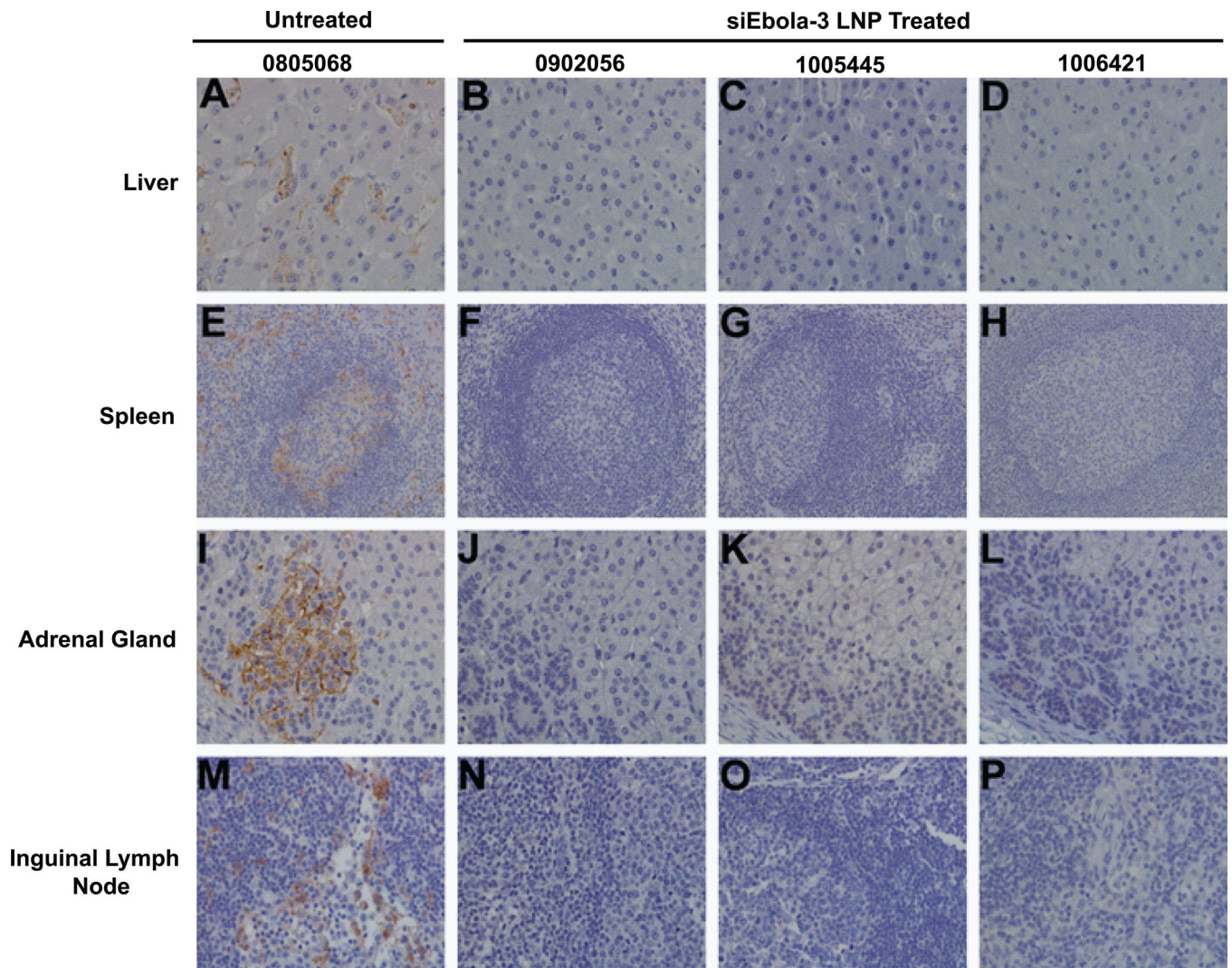


**Figure 3. EBOV Makona tissue pathology and antigen in NHPs untreated or treated with siEbola-3 LNP**

**a.** Immunolabeling of sinusoidal lining and Kupffer cells in untreated animal. **b, c, d.** No immunolabeling of treated animals. **e.** Immunolabeling of dendriform mononuclear cells in red and white pulp of untreated animal. **f, g, h.** No immunolabeling of treated animals. **i.** Immunolabeling of cortical and interstitial cells in untreated animal. **j, k, l.** No immunolabeling of treated animals. **m.** Immunolabeling, dendriform mononuclear cells within subcapsular and medullary sinuses in untreated animal. **n, o, p.** No immunolabeling of treated animals.

**Table 1**

Clinical description and outcome of EBOV-challenged NHPs

Subject No.	Sex	Group	Clinical illness	Clinical pathology
0805068	M	Untreated Control	Fever (d6); mild depression (d6–7); severe depression (d8); lethargy (d7–8); loss of appetite (d6–8); mild petechial rash (d8); rectorrhagia (d8); hunched posture (d6,7,8 am); recumbency (d8 pm); Animal euthanized in pm on d8	Leukocytosis (d6,8); granulocytosis (d3,6,8); thrombocytopenia (d6,8); lymphopenia (d3,6,8); ALT >10-fold ↑ (d8); AST >4-fold ↑ (d6); AST >10-fold ↑ (d8); ALP >2-fold ↑ (d6); ALP >8-fold ↑ (d8); GGT >10-fold ↑ (d8); BUN >8-fold ↑ (d8); CRE 7-fold ↑ (d8); CRP >10-fold ↑ (d6,8); fibrinogen >2-fold ↑ (d6)
1105274	F	Untreated Control	Fever (d6–7), mild depression (d8); severe depression (d9); lethargy (d8–9); loss of appetite (d8–9); mild petechial rash (d9); diarrhea (d9); hunched posture (d9 am); recumbency (d9 pm); Animal euthanized in pm on d9	Leukocytosis (d6); granulocytosis (d6); thrombocytopenia (d9); ALT >6-fold ↑ (d9); AST >10-fold ↑ (d9); BUN >2-fold ↑ (d9); CRP >10-fold (d6); 4-fold ↑ (d9); APTT >2-fold ↑ (d9); fibrinogen >2-fold ↑ (d6)
JE60	M	Untreated Control	Fever (d6), mild to moderate depression (d6–8); severe depression (d9); lethargy (d7–9); loss of appetite (d6–9); mild petechial rash (d6–9); severe epistaxis (d9); diarrhea (d9); hunched posture (d6–8); recumbency (d9); Animal euthanized in am on d9	Thrombocytopenia (d6,9); lymphopenia (d6,9); hypoalbuminemia (d9); hypoproteinemia (d9); AST >6-fold ↑ (d9); BUN >2-fold ↑ (d9); CRP >10-fold (d6); 4-fold ↑ (d9); APTT >2-fold ↑ (d9)
0902056	F	72 h Delay to treat	Fever (d8–10); mild depression (d8–12); loss of appetite (d5–13); mild petechial rash (d9–15); Animal survived	Leukocytosis (d10); granulocytosis (d6,10); thrombocytopenia (d6,10,14); lymphopenia (d6); ALT >2-fold ↑ (d6,10); AST >4-fold ↑ (d6); AST >10-fold ↑ (d10); GGT >2-fold ↑ (d10); CRP > 10-fold ↑ (d6,10); fibrinogen >2-fold ↑ (d6)
1005445	M	72 h Delay to treat	Mild depression (d8–12); loss of appetite (d5–14); mild petechial rash (d9–13); Animal survived	Granulocytosis (d10); Thrombocytopenia (d6,10); lymphopenia (d6); ALT >10-fold ↑ (d6); ALT >5-fold ↑ (d10); AST >10-fold ↑ (d6,10); CRP > 10-fold ↑ (d6,10); APTT >3-fold ↑ (10)
1006241	M	72 h Delay to treat	Fever (d5–7); mild depression (d8–11); loss of appetite (d7–14); Animal survived	Leukocytosis (d6,14); granulocytosis (d6,14); AST >7-fold ↑ (d10); CRP > 10-fold ↑ (d6,10) fibrinogen >2-fold ↑ (d6)

<sup>a</sup>Days after EBOV challenge are in parentheses. Fever is defined as a temperature more than 2.5°F over baseline or at least 1.5°F over baseline and 103.5°F. Mild rash: focal areas of petechiae covering less than 10% of the skin. Lymphopenia and thrombocytopenia are defined by a 40% drop in numbers of lymphocytes and platelets, respectively. Leukocytosis and granulocytosis are defined by 40% increase in numbers of white blood cells. (ALP) alkaline phosphatase, (ALT) alanine aminotransferase, (AST) aspartate aminotransferase, (APTT) activated partial thromboplastin time, (BUN) blood urea nitrogen, (CRE) creatinine, (CRP) C-reactive protein, (GGT) gamma glutamyltransferase.